Combination of results on the Higgs Boson in ATLAS

Bruno Mansoulié, on behalf of the ATLAS Collaboration
DSM-IRFU-SPP, CEA Saclay, 91191 Gif-sur-Yvette CEDEX France

The combination of the most recent results obtained by the ATLAS experiment at the LHC on the Higgs boson is presented. The combined mass measurement derived from the $H\to\gamma\gamma$ and $H\to ZZ^{(*)}\to 4\ell$ channels using the full 2011 and 2012 dataset is $m_H = 125.5 \pm 0.2\,(\text{stat})\,^{+0.5}_{-0.6}\,(\text{sys})$ GeV. The combination of all studied final states, including the $H\to\tau\tau$, $H\to b\bar{b}$, and $H\to WW^{(*)}\to\ell\nu\ell\nu$ channels using a partial dataset is reported. The combined signal strength is determined to be $\mu = 1.43 \pm 0.16\,(\text{stat}) \pm 0.14\,(\text{sys})$ at a mass of 125.5 GeV. The production modes and coupling properties of this new particle are also studied.

1 Introduction

The observation of a new particle in the search for the Standard Model (SM) Higgs boson at the LHC, reported by the ATLAS [1] and CMS [2] Collaborations, is a milestone in the quest to understand electroweak symmetry breaking[3,4,5]. In Refs. [1,6] the ATLAS Collaboration reported first measurements of the mass of this particle and its coupling properties. Updated results are presented at this conference, for the bosonic decay modes [7] and the fermionic ones [8]. This document presents an update of the combined measurements of the mass and signal strength of the observed new particle[9], including the updated analyses of $H\to\gamma\gamma$[10] and $H\to ZZ^{(*)}\to 4\ell$[11] using about $4.8\,\text{fb}^{-1}$ of pp collision data at $\sqrt{s} = 7$ TeV and $20.7\,\text{fb}^{-1}$ at $\sqrt{s} = 8$ TeV . The measured yields are analysed in terms of the signal strengths, for different production and decay modes and for their combination. Finally the couplings of the newly discovered boson are probed with fits to the observed data under several assumptions.

2 Statistical method

The results are based on the same statistical model as in Refs. [1,6]. A parameter of interest (or vector of parameters) $\boldsymbol{\mu}$ is estimated by maximizing a profile likelihood function:

$$\Lambda(\boldsymbol{\mu}) = \frac{L\big(\boldsymbol{\mu}, \hat{\hat{\boldsymbol{\theta}}}(\boldsymbol{\mu})\big)}{L(\hat{\boldsymbol{\mu}}, \hat{\boldsymbol{\theta}})} \tag{1}$$

where $\boldsymbol{\theta}$ represents the vector of nuisance parameters. In the denominator both $\boldsymbol{\mu}$ and $\boldsymbol{\theta}$ have been adjusted to find the global maximum of the likelihood function L. Their best-fit values are noted $\hat{\boldsymbol{\mu}}$, $\hat{\boldsymbol{\theta}}$. In the numerator, for a chosen $\boldsymbol{\mu}$, the nuisance parameters $\boldsymbol{\theta}$ are adjusted to maximize L, and their value is then noted $\hat{\hat{\boldsymbol{\theta}}}$. The ratio $\Lambda(\boldsymbol{\mu})$ is then a function of the parameter(s) of interest $\boldsymbol{\mu}$, and asymptotically, the test statistic $-2\ln\Lambda(\boldsymbol{\mu})$ follows a χ^2 distribution with n degrees of freedom ($\mu_{1,\ldots,n}$).

In the model, one must provide the probability distribution functions (pdf) of the nuisance parameters associated with sources of systematic uncertainty. These pdf's are most often taken as Gaussian, Log Normal (for positive variables), or Poisson (for discrete values), as they result from the effect of several statistical contributions. However, for some systematic uncertainties it is useful to consider a *rectangular* pdf (flat distribution over an interval), for example when the nuisance parameter is only known to be constrained between two bounds.

3 Mass systematic uncertainties

For the $H\to ZZ^{(*)}\to 4\ell$ decay mode, the mass measurement is dominated by the 4 muon decay channel, which has the best resolution and lowest background. In this channel, the mass-scale uncertainty comes from the muon momentum scale uncertainty, estimated to be 0.2% from the study of J/ψ, Υ and Z samples. For the decay modes containing electrons, the mass-scale uncertainty is related to the electron energy scale uncertainty, which will be described below.

For the $H\to\gamma\gamma$ decay mode, the mass scale uncertainties, coming from the photon energy scale uncertainties, can be separated into two classes. In the first class, the uncertainties must be determined for each of the analysis categories used in the $H\to\gamma\gamma$ analysis. These mainly include: the method uncertainty (0.3%, mainly the extraction of the energy scale from $Z\to ee$), the uncertainty related to the amount of material in front of the calorimeter (0.3%) and the relative calibration of the presampler detector in front of the calorimeter (0.1%). Each of the above uncertainties receives contributions from two components: the extrapolation in energy from that of electrons in $Z\to ee$ to the measured photon energy, and the transfer of the electron calibration to the photon calibration. The second class contains uncertainties which can be estimated for the whole photon sample irrespective of the analysis category. These contain the ratio of the first to second calorimeter sampling energies, the lateral leakage of showers, the fraction of conversions, etc., and amount to $\sim 0.32\%$. The overall systematic uncertainty on mass scale for the $H\to\gamma\gamma$ mode is 0.55% or 0.7 GeV.

4 Mass measurement

4.1 Combined mass determinations from the $H\to\gamma\gamma$ and $H\to ZZ^{(*)}\to 4\ell$ channels

In the $H\to\gamma\gamma$ and $H\to ZZ^{(*)}\to 4\ell$ channels the final state can be fully reconstructed with an excellent mass resolution. The results from these two analyses for the full 2011 and 2012 data samples are combined, corresponding to integrated luminosities of about $4.8\,\text{fb}^{-1}$ at $\sqrt{s}=7$ TeV and $20.7\,\text{fb}^{-1}$ at $\sqrt{s}=8$ TeV. The combination uses a common value of the Higgs boson mass, m_H, as the parameter of interest, leaving free the signal strengths of each mode. Figure 1 shows the profile likelihood ratio as a function of m_H for the $H\to\gamma\gamma$ and $H\to ZZ^{(*)}\to 4\ell$ channels and their combination. The combined mass is measured to be

$$m_H = 125.5 \pm 0.2\,(\text{stat})\,^{+0.5}_{-0.6}\,(\text{sys})\ \text{GeV}\ . \tag{2}$$

4.2 Consistency of the mass determinations from $H\to\gamma\gamma$ and $H\to ZZ^{(*)}\to 4\ell$

For the previous combination reported in Ref. [12] the compatibility of the two mass measurements was 0.8% (2.7σ). To assess the consistency of the updated measurements, a likelihood function

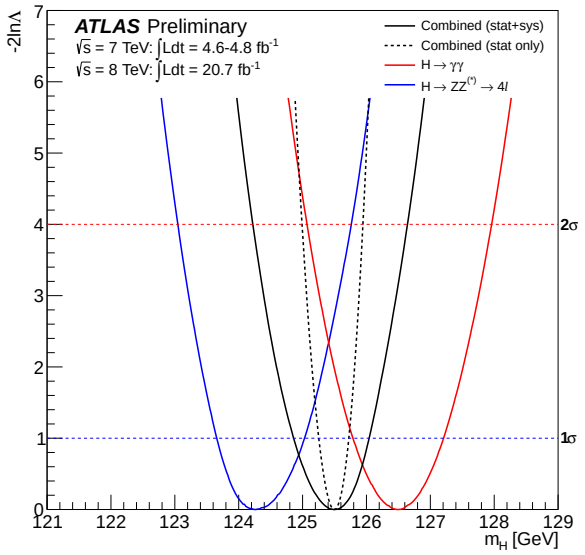

Figure 1: The profile likelihood ratio $-2\ln\Lambda(m_H)$ as a function of m_H for the $H\to\gamma\gamma$ and $H\to ZZ^{(*)}\to 4\ell$ channels and their combination, obtained by allowing the signal strengths $\mu_{\gamma\gamma}$ and $\mu_{4\ell}$ to vary independently. The dashed line shows the statistical component of the mass measurement uncertainty . From Ref. 9.

in which the mass parameters $m_H^{\gamma\gamma}$ and $m_H^{4\ell}$ vary independently is considered first. Figure 2(a) shows likelihood contours in $m_H^{\gamma\gamma}$ and $m_H^{4\ell}$ around the two best-fit mass values and the line defined by $m_H = m_H^{\gamma\gamma} = m_H^{4\ell}$.

The measurements are slightly correlated, due to the common e/γ energy scale from the $Z\to e^+e^-$ based calibration between the $H\to\gamma\gamma$ mode and $H\to ZZ^{(*)}\to 4\ell$ with electrons in the final state. Indeed, the mass consistency between the muon and electron final states in the $H\to ZZ^{(*)}\to 4\ell$ channel causes a $\sim 0.8\sigma$ adjustment in the overall e/γ energy scale which induces an approximate 350 MeV downward shift of $m_H^{\gamma\gamma}$ in the combination, with respect to the value measured from this channel alone. To quantify the consistency between the measured $m_H^{\gamma\gamma}$ and $m_H^{4\ell}$ values, a likelihood function $\Lambda(\Delta m_H)$ is considered for the mass difference $\Delta m_H = m_H^{\gamma\gamma} - m_H^{4\ell}$, with the average mass m_H profiled in the fit. This allows the hypothesis $\Delta m_H = 0$ to be tested. The signal strengths $\mu_{\gamma\gamma}$ and $\mu_{4\ell}$ are again treated as independent nuisance parameters. The likelihood is shown in Figure 2(b) as a function of the mass difference. The estimated $H\to\gamma\gamma$ and $H\to ZZ^{(*)}\to 4\ell$ mass difference is

$$\Delta\hat{m}_H = 2.3^{+0.6}_{-0.7}\,(\text{stat})\ \pm 0.6\,(\text{sys})\ \ \text{GeV}\ . \tag{3}$$

The mass difference is reduced with respect to the one reported in Ref. [12] by about 700 MeV. This reduction is driven by changes in the individual measurements reported in Refs. [10,11] where the compatibility with the previously measured values is discussed.

From the value of the likelihood evaluated at $\Delta m_H = 0$, indicated in Figure 2(b), the probability for a single Higgs-like boson to produce a value of the $\Lambda(\Delta m_H)$ test statistic disfavoring the $\Delta m_H = 0$ hypothesis by more than observed in the data is found to be at the level of 1.2% (2.5σ) using the asymptotic approximation assumption, and 1.5% (2.4σ) using Monte Carlo ensemble tests.[a] Further checks, assuming the SM signal strengths for $H\to\gamma\gamma$ and $H\to ZZ^{(*)}\to 4\ell$ or constraining the ensemble of pseudo-experiments to the observed signal strengths, yield similar probabilities, since μ and m_H are largely uncorrelated.

The significance of the mass difference is also tested using rectangular pdfs for the systematic energy scale uncertainties coming from the $Z\to ee$ calibration method, the imperfect knowledge of the material upstream of the electromagnetic calorimeter and the energy scale of the presampler detector. The rectangular pdfs correspond to a uniform *a priori* likelihood in the range of

[a] Here 2-sided probabilities are used as both cases, $m_H^{\gamma\gamma} > m_H^{4\ell}$ and $m_H^{\gamma\gamma} < m_H^{4\ell}$, are considered.

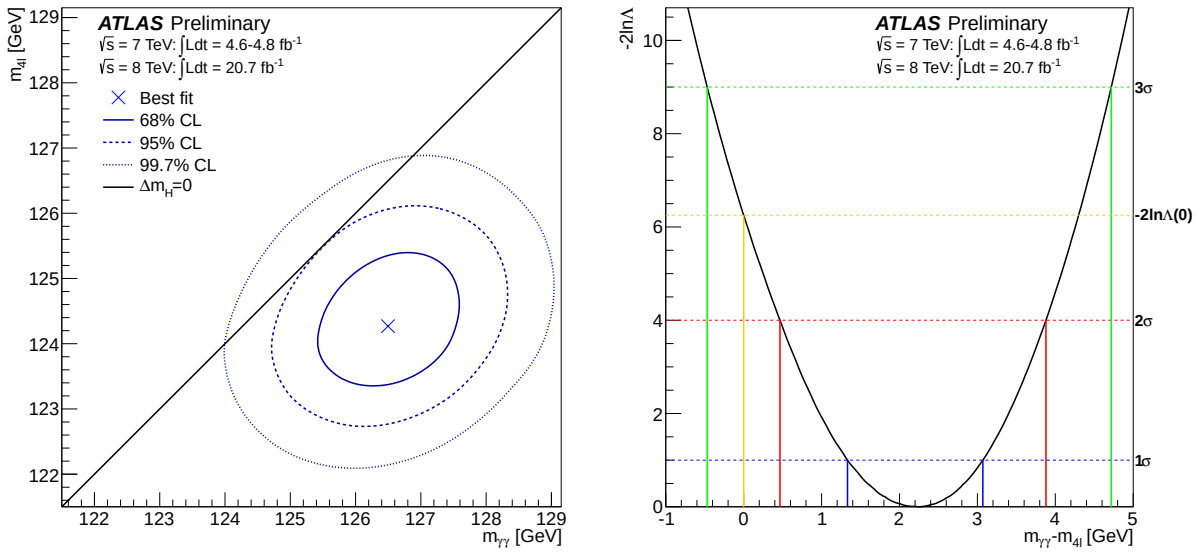

(a) (b)

Figure 2: (a) Likelihood contours as a function of $m_H^{\gamma\gamma}$ and $m_H^{4\ell}$. (b) Likelihood as a function of the mass difference, $\Delta m_H = m_H^{\gamma\gamma} - m_H^{4\ell}$, profiling over the common mass m_H. In both cases the signal strength parameters $\mu_{\gamma\gamma}$ and $\mu_{4\ell}$ are allowed to vary independently. In (a) the masses are considered as two independent parameters of interest (2-dimensional contours) while in (b) only one parameter of interest, the mass difference, is considered (1-dimensional variation of the likelihood). From Ref. 9.

the $\pm 1\sigma$ Gaussian uncertainty intervals for these three sources of systematic uncertainties and a zero probability outside the $\pm 1\sigma$ range. With this treatment of these energy scale systematic uncertainties, the probability for a single Higgs-like boson to produce a value of the $\Lambda(\Delta m_H)$ test statistic disfavoring the $\Delta m_H = 0$ hypothesis by more than observed in the data is found to be 8%.,

5 Signal production strength

Signal strength parameters μ are defined as the yield divided by the corresponding SM value. The best-fit signal strength parameter $\hat{\mu}$ is a convenient observable to test the compatibility of the data with the background-only hypothesis ($\mu = 0$) and the SM Higgs hypothesis ($\mu = 1$). Hypothesized values of the global signal strength parameter μ and the strength parameters for each channel μ_i are tested with the statistic $\Lambda(\boldsymbol{\mu})$ as defined in Eqn. 1. This test statistic extracts the information on the parameters of interest from the full likelihood function, assuming a fixed, common, m_H. The best-fit values of the signal strength parameter for each channel independently and for the combination are given in Fig. 3 for the measured combined mass $m_H = 125.5$ GeV. The observed yield corresponds to a measured signal strength of $1.43 \pm 0.16\,(\text{stat}) \pm 0.14\,(\text{sys})$ for $m_H = 125.5$ GeV with all channels combined. This combined signal strength is consistent with the SM Higgs boson hypothesis $\mu = 1$ at the 3% level. Alternatively, the consistency with the SM Higgs boson hypothesis is also tested using rectangular pdfs for the dominant theory systematic uncertainties from $gg \to H$ QCD scale and parton density functions variations following the recommendations in Refs. [13,14]. With this treatment the consistency of the observed signal strength with the SM hypothesis is increased to ∼11%. A compatibility test between the signal strengths of the five channels and the Standard Model expectation of unity for all channels gives a probability of about 8%. The compatibility between the combined best-fit signal strength $\hat{\mu}$ and the best-fit signal strengths of the five channels is 32%. The dependence of the combined value of $\hat{\mu}$ on the assumed m_H has been investigated and is relatively weak: changing the mass hypothesis between 124.5 and 126.5 GeV changes the value of $\hat{\mu}$ by about

4%.

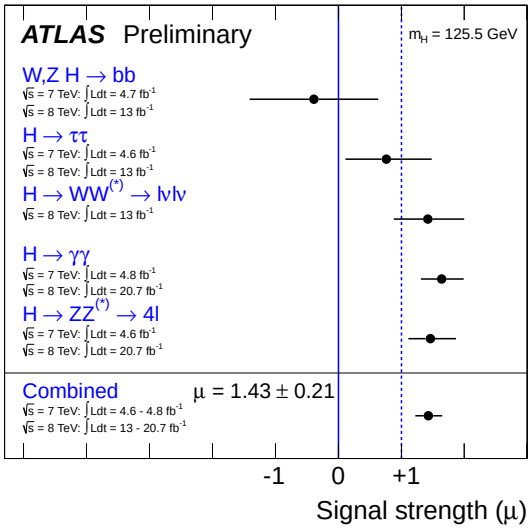

Figure 3: Measurements of the signal strength parameter μ for m_H =125.5 GeV for the individual channels and for their combination. From Ref. 9.

In order to test which values of signal strength and Higgs mass are simultaneously consistent with the data for the $H\to\gamma\gamma$ and $H\to ZZ^{(*)}\to 4\ell$ channels, the profile likelihood ratio $\Lambda(\mu, m_H)$ is used. The resulting 68% and 95% confidence level (CL) contours are shown in Fig. 4.

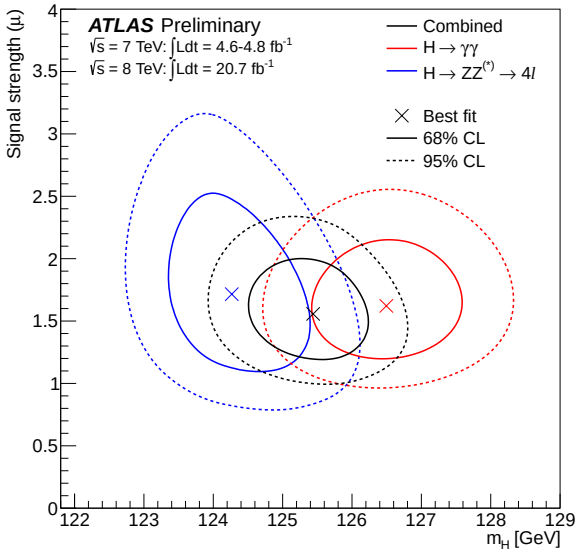

Figure 4: Confidence level intervals in the (μ, m_H) plane for the $H\to ZZ^{(*)}\to 4\ell$ and $H\to\gamma\gamma$ channels and their combination, including all systematic uncertainties. The markers indicate the maximum likelihood estimates $(\hat{\mu}, \hat{m}_H)$ in the corresponding channels. From Ref. 9.

6 Production modes

The dominant production mode of the Standard Model Higgs boson is gluon-fusion, but it is important to search for evidence for the Vector Boson Fusion (VBF) mode. The modes $q\bar{q}/gg \to t\bar{t}H$ and $q\bar{q} \to WH/ZH$ are expected to provide very small contributions with the present statistics. Hence μ_{ggH} and μ_{ttH} have been grouped together as they scale dominantly with the ttH coupling in the SM and are denoted by the common parameter $\mu_{ggF+ttH}$. Similarly,

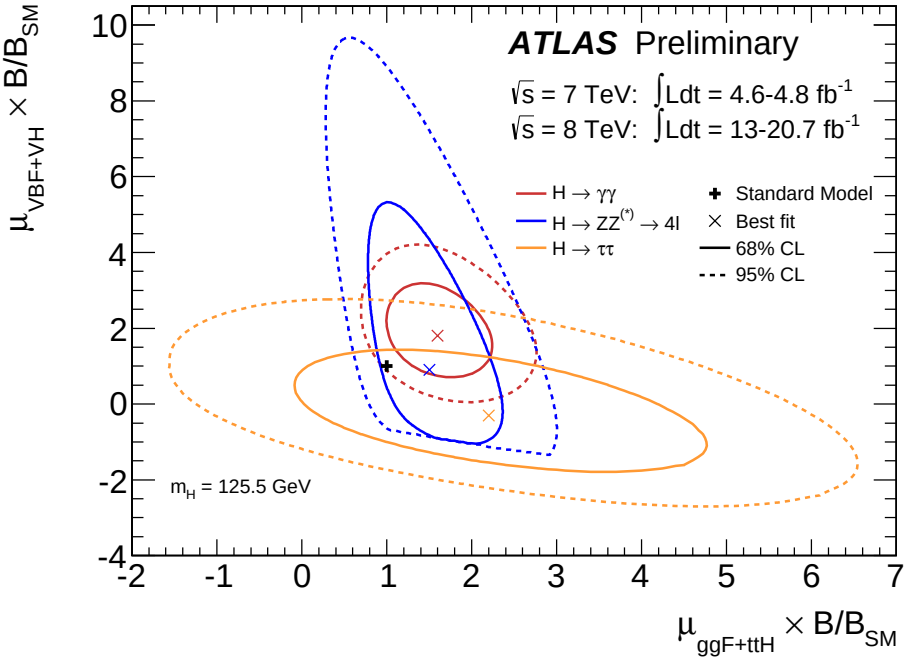

Figure 5: Likelihood contours for the $H\to\gamma\gamma$, $H\to ZZ^{(*)}\to 4\ell$ and $H\to\tau\tau$ channels in the $(\mu_{\mathrm{ggF}+t\bar{t}H}, \mu_{\mathrm{VBF}+VH})$ plane for a Higgs boson mass hypothesis of $m_H = 125.5$ GeV. Both $\mu_{\mathrm{ggF}+t\bar{t}H}$ and $\mu_{\mathrm{VBF}+VH}$ are modified by the branching ratio factor B/B_{SM}, which can be different for the different final states. The quantity $\mu_{\mathrm{ggF}+t\bar{t}H}$ ($\mu_{\mathrm{VBF}+VH}$) is a common scale factor for the gluon-fusion and $t\bar{t}H$ (VBF and VH) production cross sections. The best-fit to the data (×) and 68% (full) and 95% (dashed) CL contours are also indicated, as well as the SM expectation (+). From Ref. 9.

μ_{VBF} and μ_{VH} have been grouped together as they scale with the WH/ZH coupling in the SM and are denoted by the common parameter μ_{VBF+VH}. The resulting contours for the $H\to\gamma\gamma$, $H\to ZZ^{(*)}\to 4\ell$ and $H\to\tau\tau$ channels, each using analysis categories optimized for the measurement of VBF Higgs production, are shown in Fig. 5 for m_H=125.5 GeV.

It should be noted that the factors μ_f, the ratio of the branching ratio in a given final state f to the SM one may have different values for different decay modes, hence a direct comparison of the results among different final states is not possible. Such comparisons need consistent coupling modifications in the initial and final state. It is possible, however, to use ratios to eliminate the dependence on the branching fractions and illustrate the relative discriminating power between ggH+ttH and VBF+VH, as well as the compatibility of the measurements across channels. The likelihood as a function of the ratio $\mu_{\mathrm{VBF}+VH}/\mu_{\mathrm{ggF}+t\bar{t}H}$ is shown for the $H\to\gamma\gamma$, $H\to ZZ^{(*)}\to 4\ell$ and $H\to\tau\tau$ channels and their combination in Fig. 6. The measurements in the three channels as well as the observed combined ratio of $\mu_{\mathrm{VBF}+VH}/\mu_{\mathrm{ggF}+t\bar{t}H} = 0.9^{+0.7}_{-0.4}$ are compatible with the SM expectation of unity.

7 Couplings

A relative coupling κ_i is defined as the ratio of the measured coupling to the SM one. For each observed final state of the SM Higgs boson, the production and decay rates involve several couplings. For example in the $H\to\gamma\gamma$ mode, the production rate from gluon-fusion is proportional to the effective Higgs-gluon coupling ${\kappa_g}^2$, where κ_g is itself a function of the Higgs couplings to the top κ_t and to the bottom κ_b, and m_H. The production rate from VBF depends on ${\kappa_W}^2$. The decay rate is proportional to $(\kappa_W - 0.2\kappa_t)^2$, with an interference between the top and W loops. Consequently, the elementary couplings of the Higgs to the different particles cannot be derived directly from the observed rates, but need a consistent parametrization, as proposed by

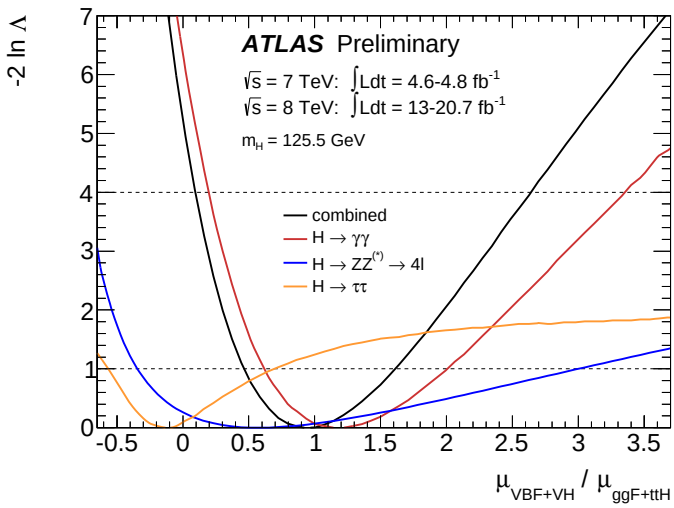

Figure 6: Likelihood curves for the ratio $\mu_{\mathrm{VBF}+VH}/\mu_{\mathrm{ggF}+t\bar{t}H}$ from the $H\to\gamma\gamma$, $H\to ZZ^{(*)}\to 4\ell$ and $H\to\tau\tau$ channels, and their combination, for a Higgs boson mass hypothesis of $m_H = 125.5$ GeV. The branching ratios, and possible non-SM effects affecting them, cancel in the ratio $\mu_{\mathrm{VBF}+VH}/\mu_{\mathrm{ggF}+t\bar{t}H}$, hence the different measurements from all three channels can be compared and combined. From Ref. 9.

the LHC Cross Section Working Group[15]. Ideally, the measurement of all production and decay modes would allow to derive all the couplings, but in practice some modes are inaccessible. It is then necessary to group some couplings into consistent models to test the most important features of the newly found boson against the SM Higgs hypothesis.

7.1 Fermion versus Vector couplings

In this model, all fermion couplings are taken equal under $\kappa_F = \kappa_t = \kappa_b = \kappa_\tau$, and all vector couplings are taken equal under $\kappa_V = \kappa_W = \kappa_Z$. The model assumes that gluon-fusion production and $H\to\gamma\gamma$ decay occur only through loops of SM particles. Figure 7 shows the corresponding likelihood contours of the data in the κ_V, κ_F plane. Only the relative sign of κ_V and κ_F is relevant, and the sign of κ_V is chosen positive. The degeneracy between the two possible minima can only be lifted by the interference term in the $H\to\gamma\gamma$ decay mode. The present data slightly favours the SM minimum. The (2D) compatibility of the SM hypothesis with the best fit is 21%. With this data, the sensitivity to κ_F is mostly through the coupling to the top involved in the loops. It will be much better with the forthcoming results of the $b\bar{b}$ and $\tau\tau$ modes.

7.2 W and Z couplings (custodial symmetry)

Identical coupling scale factors for the W and Z are an important ingredient of the Standard Model, often referred to as custodial symmetry. In the previous model, κ_W and κ_Z are now separated, and their ratio λ_{WZ} is probed. Figure 8 shows the likelihood distribution for λ_{WZ}. The measured value is $\lambda_{WZ} = 1.07^{+0.35}_{-0.27}$.

7.3 Contribution from non-SM particles

This model assumes that all couplings to SM particles have their standard value, *i.e.* $\kappa_i = 1$, but the effective couplings to gluon and photon, κ_g and κ_γ are taken as independent, allowing for additional contributions from new particles in the gluon-fusion production and $H\to\gamma\gamma$ decay diagram loops. As a first step, the model assumes that these particles do not contribute to the total width through undetected modes. Figure 9 shows the likelihood contours in the κ_g , κ_γ plane. The best fit values, profiling over the other parameter, are $\kappa_g = 1.1^{+0.2}_{-0.3}$ and $\kappa_\gamma = 1.2^{+0.3}_{-0.2}$.

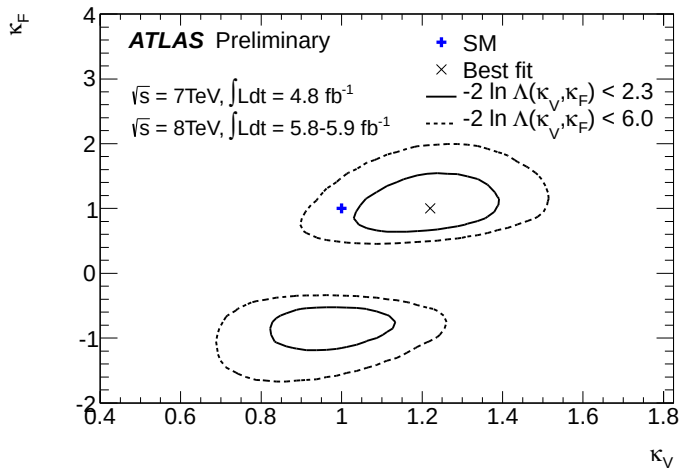

Figure 7: Likelihood contours of the coupling scale factors κ_F and κ_V for a 2-parameter benchmark model probing different coupling strength scale factors for fermions and vector bosons, assuming no non-SM contribution to the total width. From Ref. 6.

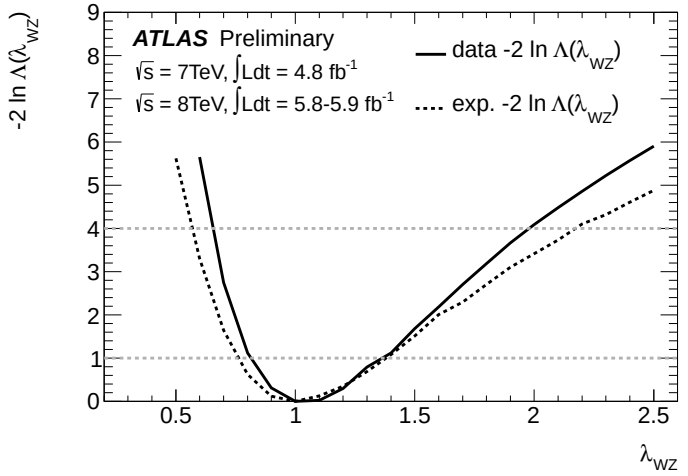

Figure 8: Likelihood distribution of $\lambda_{WZ} = \kappa_W/\kappa_Z$ for a benchmark model probing the custodial symmetry with independent κ_F, κ_W, κ_Z. From Ref. 6.

The compatibility of the SM hypothesis (2D) with the best fit point is 18%. In a second step, the assumption on the total width is released. The free parameters are κ_g, κ_γ and $BR_{inv.,undet.}$, where the latter represents the branching ratio to possible invisible and undetected decay modes. Profiling over κ_g and κ_γ, the 68% CL (resp. 95%) upper limits on $BR_{inv.,undet.}$ are found to be 0.68 (resp. 0.84).

8 Conclusion

An update of the properties of the newly discovered Higgs-like boson using the dataset corresponding to about $4.8\,\text{fb}^{-1}$ of pp collision data recorded by ATLAS at $\sqrt{s} = 7$ TeV and up to $20.7\,\text{fb}^{-1}$ recorded at $\sqrt{s} = 8$ TeV is presented. The measured mass, based on the high mass resolution channels $H\to\gamma\gamma$ and $H\to ZZ^{(*)}\to 4\ell$, is $m_H = 125.5\pm0.2\,(\text{stat})\,^{+0.5}_{-0.6}\,(\text{sys})$ GeV. The measurements of the signal strengths for the final states $H\to\gamma\gamma$, $H\to ZZ^{(*)}\to 4\ell$, $H\to WW^{(*)}\to\ell\nu\ell\nu$, $H\to\tau\tau$ and $H\to b\bar{b}$ have been combined, giving an average value of $1.43\pm0.16\,(\text{stat})\pm0.14\,(\text{sys})$ obtained at the mass of 125.5 GeV. A compatibility test between this combined signal strength and the Standard Model expectation of unity gives a probability of about 3%. A more conserva-

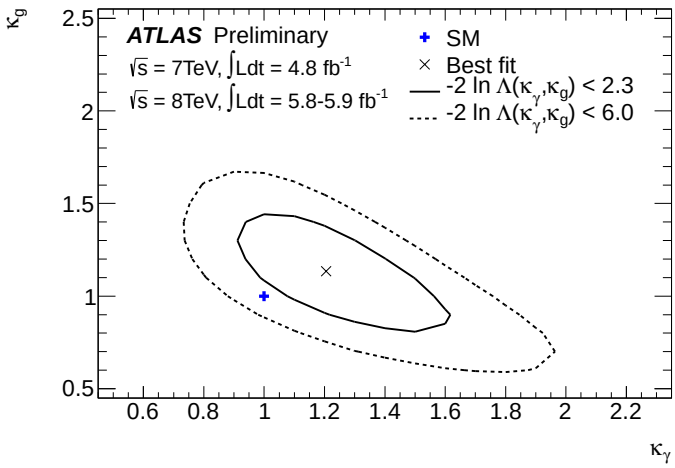

Figure 9: Likelihood contours for a benchmark model probing for contributions from non-SM particles in the $gg \to H$ and $H \to \gamma\gamma$ loops, assuming no sizable extra contribution to the total width. From Ref. 6.

tive treatment of the $gg \to H$ related theory systematic uncertainty, using rectangular pdfs for the QCD scale and PDF related errors, improves the compatibility to the level of ∼11%. The measured cross section ratio between vector boson mediated and gluon (top) mediated Higgs boson production is found to be $\mu_{\mathrm{VBF}+VH}/\mu_{\mathrm{ggF}+t\bar{t}H} = 0.9^{+0.7}_{-0.4}$. The couplings of the new particle, studied on a partial dataset with simplified benchmark models, are found to be in agreement with that of the SM Higgs boson.

References

1. ATLAS Collaboration. Observation of a new particle in the search for the Standard Model Higgs boson with the ATLAS detector at the LHC. *Phys. Lett.*, B 716:1–29, 2012.
2. CMS Collaboration. Observation of a new boson at a mass of 125 GeV with the CMS experiment at the LHC. *Phys. Lett.*, B 716:30–61, 2012.
3. F. Englert and R. Brout. Broken symmetry and the mass of gauge vector mesons. *Phys. Rev. Lett.*, 13:321–323, 1964.
4. Peter W. Higgs. Broken symmetries and the masses of gauge bosons. *Phys. Rev. Lett.*, 13:508–509, 1964.
5. G. S. Guralnik, C. R. Hagen, and T. W. .B. Kibble. Global conservation laws and massless particles. *Phys. Rev. Lett.*, 13:585–587, 1964.
6. ATLAS Collaboration. Coupling properties of the new Higgs-like boson observed with the ATLAS detector at the LHC. *ATLAS-CONF-2012-127*. https://cds.cern.ch/record/1476765.
7. F. Hubault. *These proceedings.*
8. V. Martin. *These proceedings.*
9. ATLAS Collaboration. Combined measurements of the mass and signal strength of the Higgs-like boson with the ATLAS detector using up to 25 fb^{-1} of proton-proton collision data. *ATLAS-CONF-2013-014*, 2013. https://cds.cern.ch/record/1523727.
10. ATLAS Collaboration. Measurements of the properties of the Higgs-like boson in the two photon decay channel with the ATLAS detector using 25 fb^{-1} of proton-proton collision data. *ATLAS-CONF-2013-012*. https://cds.cern.ch/record/1523698.
11. ATLAS Collaboration. Measurements of the properties of the Higgs-like boson in the four lepton decay channel with the ATLAS detector using 25 fb^{-1} of proton-proton collision data. *ATLAS-CONF-2013-013*. https://cds.cern.ch/record/1523699.
12. ATLAS Collaboration. An update of combined measurements of the new Higgs-like boson

with high mass resolution channels. *ATLAS-CONF-2012-170*. https://cds.cern.ch/record/1499629.
13. LHC Higgs Cross Section Working Group, S. Dittmaier, C. Mariotti, G. Passarino, and R. Tanaka (Eds.). Handbook of LHC Higgs cross sections: 1. Inclusive observables. *CERN-2011-002*, CERN, Geneva, 2011.
14. LHC Higgs Cross Section Working Group, S. Dittmaier, C. Mariotti, G. Passarino, and R. Tanaka (Eds.). Handbook of LHC Higgs Cross Sections: 2. Differential Distributions. *CERN-2012-002*, CERN, Geneva, 2012.
15. LHC Higgs Cross Section Working Group, A. David *et al.* LHC HXSWG interim recommendations to explore the coupling structure of a Higgs-like particle. 2012.